ACS Catalysis

Research Article

pubs.acs.org/acscatalysis

Understanding the Effect of the Adatoms in the Formic Acid Oxidation Mechanism on Pt(111) Electrodes

Adolfo Ferre-Vilaplana,[†,‡] Juan Víctor Perales-Rondón,[§] Juan M. Feliu,[§] and Enrique Herrero*[,§]

[†]Instituto Tecnológico de Informática, Ciudad Politécnica de la Innovación, Camino de Vera s/n, E-46022 Valencia, Spain

[‡]Departamento de Sistemas Informáticos y Computación, Escuela Politécnica Superior de Alcoy, Universidad Politécnica de Valencia, Plaza Ferrándiz y Carbonell s/n, E-03801 Alcoy, Spain

[§]Instituto de Electroquímica, Universidad de Alicante, Apdo. 99, E-03080 Alicante, Spain

ABSTRACT: The engineered search for new catalysts requires a deep knowledge about reaction mechanisms. Here, with the support of a combination of computational and experimental results, the oxidation mechanism of formic acid on Pt(111) electrodes modified by adatoms of the p block is elucidated for the first time. DFT calculations reveal that some adatoms, such as Bi and Pb, have positive partial charge when they are adsorbed on the bare surface, whereas others, such as Se and S, remain virtually neutral. When the partial charge is correlated with previously reported experimental results for the formic acid oxidation reaction, it is found that the partial positive charge is directly related to the increase in catalytic activity of the modified surface. Further, it is obtained that such a positive partial charge is directly proportional to the electronegativity difference between the adatom and Pt. Thus, the electronegativity difference can be used as an effective descriptor for the expected electrocatalytic activity. This partial positive charge on the adatom drives the formic acid oxidation reaction, since it favors the formation and adsorption of formate on the adatom. Once adsorbed, the neighboring platinum atoms assist in the C−H bond cleavage. Finally, it is found that most of the steps involved in the proposed oxidation mechanism are barrierless, which implies a significant diminution of the activation barriers in comparison to that of the unmodified Pt(111) electrode. This diminution in the activation barrier has been experimentally corroborated for the Bi−Pt(111) electrode, supporting the proposed mechanism.

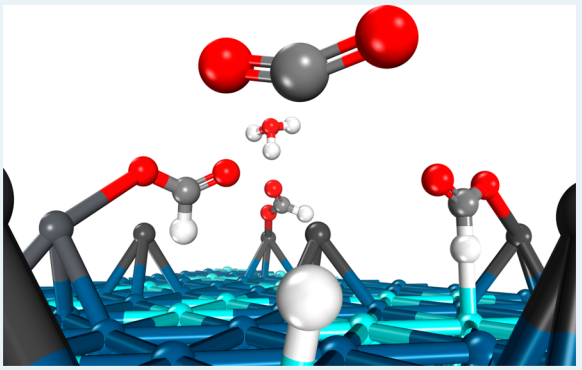

KEYWORDS: *formic acid oxidation, platinum, adatom modification, activation energy, DFT*

INTRODUCTION

The commercial exploitation of the fuel cell concept depends on the availability of new electrocatalysts capable of providing higher current densities at lower overpotentials. In the past, the search for new and better catalysts has taken place mainly by means of trial and error. However, a much more engineered searching approach, based on knowledge about reaction mechanisms and parameters determining reactivity, is increasingly feasible. A clear example of the novel approach is the recent development of new catalysts for the hydrogen oxidation reaction. For this rather simple reaction, in which two electrons are exchanged and only a single H−H bond is cleaved, it was experimentally found that the activity is related to the adsorption energy of atomic hydrogen on the catalytic metal surface.[1−3] For this reaction, when the activity is plotted versus hydrogen adsorption energy typical volcano curves are obtained,[4] from which the ideal hydrogen adsorption energy giving rise to the maximum activity can be determined. With the advent of powerful computers and methods, hydrogen adsorption energies for a large number of different alloys have been calculated, and new and more effective electrocatalysts whose energy is close to the ideal value have been identified.[5] A similar strategy has been followed for the oxygen reduction reaction, where the reactivity has been associated with the adsorption energy of different reaction intermediates.[6]

In general, the application of the exemplified engineered approach to the complete oxidation of small organic molecules to CO_2 can become much more complicated. Since several heteroatomic bonds have to be cleaved and, in many cases, even new bonds could be formed, the search for correlations between surface properties and reactivity has become much more complex. From all the small organic molecules being investigated as possible fuels, formic acid is clearly the simplest one. The complete oxidation of formic acid to yield CO_2 involves the cleavage of the O−H bond of the carboxylic group and C−H bond cleavage, giving rise to the exchange of two electrons. The first bond cleavage is rather simple, since it is related to the acid/base equilibrium of the formic acid molecule, whereas the second process requires an active metal surface. Additionally, the oxidation of the formic acid

Received: September 13, 2014
Revised: December 9, 2014
Published: December 11, 2014

DOI: 10.1021/cs501729j
ACS Catal. 2015, 5, 645−654

molecule can proceed though a second route in which adsorbed CO is formed through the cleavage of the C−H and the C−OH bonds.[7,8] Since CO is strongly adsorbed on the electrode surface, its final oxidation to CO_2 is only achieved at large overpotentials. Thus, CO can be considered as a poisoning intermediate; for this reason the formic acid oxidation route through CO should be avoided. The route yielding CO_2 without formation of CO is known as the direct route or the active intermediate route because its reaction intermediates are more easily oxidized than adsorbed CO.

Of all pure metals, platinum and palladium have the highest oxidation activity.[7] Since the formic acid oxidation reaction involves the interaction of the reactant species with the catalytic surface, a dependence of the reactivity on the surface structure has been found using platinum single-crystal electrodes.[9,10] In general, both described routes are structure sensitive and follow the same reactivity trend: i.e., the platinum surfaces that are more active for the oxidation through the active intermediate route are also more active for the CO route.[11,12] To increase the platinum activity toward the desired route and avoid CO formation, several strategies have been attempted, which involve the modification of platinum surfaces with submonolayers of different adatoms,[13−27] metallic layers,[28−30] and the preparation of intermetallic compounds with platinum.[31−35] In spite of the fact that large activity enhancements have been measured for some of the tested electrodes, especially when Bi or Pb is added, there is still no detailed explanation for the observed reactivity increase. Here we provide, for the first time, a complete and comprehensive picture of the reaction mechanism of formic acid on Pt(111) surfaces modified with adatoms of the p block, starting from a critical review of previously reported experimental results and using a combination of new experimental and computational data. Moreover, a descriptor that correlates previously reported reactivities and physical properties of the adatom has been identified. This descriptor can be used to feed future engineered searching for new catalysts.

EXPERIMENTAL AND COMPUTATIONAL METHODS

Experimental Methods. Platinum single-crystal electrodes were oriented, cut, and polished from small single-crystal beads (2.5 mm diameter) following the procedure described by Clavilier and co-workers.[36,37] The electrodes were cleaned by flame annealing, cooled under H_2/Ar, and protected with water in equilibrium with this gas mixture to prevent contamination before immersion in the electrochemical cell, as described in detail elsewhere.[37,38] The voltammetric profiles, and therefore the surface structures of the electrodes, are stable upon cycling provided that oxide formation is avoided. It is known that oxidation/reduction cycles create defects on the electrode surface.[39,40]

Bismuth adlayers were prepared by the irreversible adsorption technique. The prepared electrode surface was put in contact in a separate vessel with a solution of Bi_2O_3 (10^{-5}−10^{-4} M) in 0.1 M perchloric acid for a short period of time (5−60 s).[41] Depending on the Bi solution concentration and immersion time, different Bi coverages on the Pt(111) electrode could be obtained. The modified electrode was then rinsed with water and immersed again in the electrochemical cell. The coverage of irreversibly adsorbed bismuth was calculated using the charge of the new peak appearing in the voltammogram in 0.5 M H_2SO_4 at 0.67 V. Bismuth coverage is given as the number of Bi atoms per Pt surface atoms and has been determined according to the procedure described in ref 26. Experiments were carried out in a classical two-compartment electrochemical cell deaerated by using Ar (N50, Air Liquide in all gases used), including a large platinum counter electrode and a reversible hydrogen (N50) electrode (RHE) as reference. For the determination of the activation energy, the electrochemical cell was immersed in a water bath to control the temperature in a range between 278 and 333 K. The reference electrode was kept at room temperature (298 K), and all of the measured potentials are referenced to a RHE electrode at 298 K. For that reason, the measured potentials were corrected with the thermodiffusion potential using the procedure explained in ref 42. All potentials are quoted vs the RHE at 298 K unless otherwise stated. Solutions were prepared from sulfuric acid, perchloric acid, sodium perchlorate, acetic acid, formic acid (Merck suprapur in all cases), and ultrapure water from Elga. The cleanliness of the solutions was tested by the stability of the characteristic voltammetric features of well-defined single-crystal electrodes.

The potential program for the transients was generated with an arbitrary function generator (Rigol, DG3061A) together with a potentiostat (eDAQ, EA161) and a digital recorder (eDAQ, ED401). To avoid any interference of the diffusion of formic acid in the reaction rate, stationary conditions were attained by using a hanging meniscus rotating disk configuration at 900 rpm (controlled by a Radiometer CTV 101 instrument).

Computational Methods. All DFT calculations were carried out using numerical basis sets,[43] semicore pseudopotentials[44] (which include scalar relativistic effects), and the RPBE functional[45] as implemented in the Dmol^3 code.[46] Implicit solvation effects were taken into account by the COSMO model.[47] The effects of nonzero dipole moments in the supercells were canceled by means of external fields.[48]

The Pt(111) surface was modeled by means of a periodic supercell comprising 36 Pt atoms (four layers of metal atoms) and a vacuum slab of 20 Å. The bottom 18 Pt atoms were frozen in their bulk crystal locations. The remaining 18 Pt atoms were completely relaxed joined to the adsorbates. The shortest distance between periodic images was 8.51 Å.

Optimal configurations (adsorbent/adsorbate, reactants, products, and transition states) were searched for using numerical basis sets of double-numerical quality. During this phase of the calculations, Brillouin zones were sampled, under the Monkhorst−Pack method,[49] using grids corresponding to distances in the reciprocal space on the order of 0.05 1/Å, and convergence was facilitated introducing 0.005 Ha of thermal smearing.

Assuming the previously optimized configurations, binding energies, reaction energies, and barriers were estimated using numerical basis sets of double-numerical quality plus polarization. In this case, Brillouin zones were sampled, also under the Monkhorst−Pack method, but using grids corresponding to distances on the order of 0.04 1/Å, and convergence was facilitated introducing 0.005 Ha of thermal smearing. Moreover, energies were extrapolated to 0 K. Finally, molecular dynamic simulations were run, under the NVE thermodynamic ensemble, using the same numerical setup used for optimization calculations and 1 fs of time step.

DOI: 10.1021/cs501729j
ACS Catal. 2015, 5, 645−654

RESULTS

Critical Review of Previous Experimental Results. In a search to increase the activity of the bare surface toward the formic acid oxidation reaction, the electrocatalytic behavior of Pt(111) electrodes modified with different adatoms has been extensively investigated. Among them, the clearest example giving rise to a significant improvement in the electrocatalytic activity is probably that of bismuth.[15,26] For this modified electrode, as the adatom coverage increases, two important effects can be observed: the complete inhibition of the route through CO and a significant increase in the oxidation currents measured at low potentials. In fact, it has been reported that the dehydration path yielding CO is completely inhibited even for very low coverages.[18] Given that on the Pt(111) bare surface CO formation takes place exclusively on defect sites[50,51] and that the initial deposition stages of the bismuth adlayer also occur on the defects, very small amounts of adatom are able to completely block the CO formation reaction.[52] However, it should be stressed that this inhibition is not linked to a change in the oxidation mechanism, since no major catalytic effects are measured at small coverages.[15] Once all the defect sites have been covered, deposition starts on the well-ordered (111) domains. From these coverage levels forward, a significant increase in the catalytic activity toward CO_2 can be observed until the coverage value of 0.26 is reached.[15,26] At this optimal coverage value, measured currents for the direct oxidation of formic acid on the modified electrode at 0.5 V are ca. 15 times higher than those measured for the bare surface.[12,26] For higher coverages, the activity diminishes until the maximum stable coverage of 0.33 is obtained. At this latter coverage value, the electrocatalytic activity is almost negligible,[15] which may be explained by the fact that, at such a coverage level, all platinum sites have been covered. From the results presented above, two conclusions arise: (i) the presence of Bi on the (111) terraces catalyze the direct oxidation of formic acid to CO_2 and (ii) the availability of Pt sites seems to be a requirement for the oxidation process to take place. In fact, it has been proposed that a Pt site close to a Bi adatom would be the most catalytically active site for the considered oxidation reaction.[53] Similar conclusions have been reached for stepped surfaces with (111) terraces.[24,25] It has been shown by STM that Bi is distributed randomly over the surface, since the sizes of Bi islands on the surface are below 1 nm for low and medium coverages.[54] Assuming such a random distribution of the Bi adatom on the Pt(111) surface, a statistical model for the adatom-modified surface suggests that the Bi−Pt ensemble is the most active site for the considered reaction.[53]

For the formic acid oxidation reaction, other adatoms, such as Pb, Te, As, and Sb, on Pt(111) electrodes behave like bismuth, although with different catalytic activities.[17,19,21−23] In addition, intermetallic Pt−Pb nanoparticles display a very high electrocatalytic activity toward the considered reaction, in a way similar to that observed for Pt−Bi intermetallic nanoparticles.[33−35] Actually, the Pb−Pt(111) system displays the highest catalytic activity for the target reaction, though Pb as an adatom on the Pt(111) electrode has some stability problems, since it readily dissolves at potentials higher than 0.5 V.[19] On the other hand, certain adatoms, such as Se and S, deposited on the Pt(111) electrode do not give rise to any catalytic enhancement for the studied reaction.[20,53]

When the catalytic activities toward the target reaction of all the investigated adatom-modified Pt(111) electrodes are compared at 0.5 V, the following order can be established: Pb−Pt(111) > Bi−Pt(111) > Sb−Pt(111) > Te−Pt(111) > As−Pt(111) > Pt(111) > Se−Pt(111) = S−Pt(111). It should be emphasized that, from a practical point of view, the highest power output is always sought out for a fuel cell. Thus, when the relative performance of different electrodes is evaluated, comparison of currents at constant potential is the relevant figure. The current at peak potential is not a relevant figure for comparison because, in most of the cases, the peak potential depends on the deactivation mechanism of the surface, which can be affected by the presence of very different adsorbates such as adatoms and anions from the electrolyte.

Adatom Effect on the Pt(111) Surface. In order to understand the effect of adatoms on the bare surface, electronic structure calculations, modeling different adatom-modified Pt(111) surfaces, were carried out using DFT. Adsorption energies of adatoms on the Pt(111) surface, for both fcc and hcp sites, are summarized in Table 1. The adsorption energy of a Pt atom is also included for comparison in order to distinguish the effects related to the different chemical nature of the adatom from those related to the geometrical position of the adatom. Adatom adsorption processes give rise to electron density redistributions which are displayed in Figure 1 for fcc configurations, the results corresponding to hcp sites being very similar. As can be inferred from Figure 1, for some adatoms, such as Pb and Bi, a partial positive charge is located on the adatom, whereas the compensating negative charge is smeared out over the neighboring Pt sites. However, for other adatoms, mainly Se and S, the electron density redistribution is very small and both the adatom and the surface remain virtually neutral. To quantify the electron density changes observed upon the adsorption of the adatom, partial charges on the adatoms were estimated both under the Mulliken and Hirshfeld formalisms.[55,56] For the fcc configuration, such partial charges are summarized in Table 2. Similar values have been previously found for the Sb−Pt(111) system,[57] and similar trends have been reported for the adsorption of Bi and S on small Pt_{10} clusters.[58] From a comparison of the partial charge series with the catalytic activity sequence listed at the end of Critical Review of Previous Experimental Results, it can be concluded that there exists a clear correlation between the partial charge of the adatom and the catalytic activity of the system. Higher partial positive charge on the adatom leads to higher electrocatalytic activity toward the formic acid oxidation. Moreover, adatoms that do not have any positive partial charge such as Se and S do not exhibit any catalytic enhancement. Thus, it seems clear that the measured catalytic activity increase

Table 1. DFT Calculated Adsorption Energies of Different Adatoms Deposited on the fcc and hcp Sites of the Pt(111) Surface

	adsorption energy/eV	
	fcc	hcp
Pb	4.44	4.45
Bi	3.29	3.26
Sb	4.24	4.20
Te	3.68	3.55
As	4.40	4.33
Se	3.96	3.77
S	4.47	4.22
Pt	3.75	3.59

DOI: 10.1021/cs501729j
ACS Catal. 2015, 5, 645−654

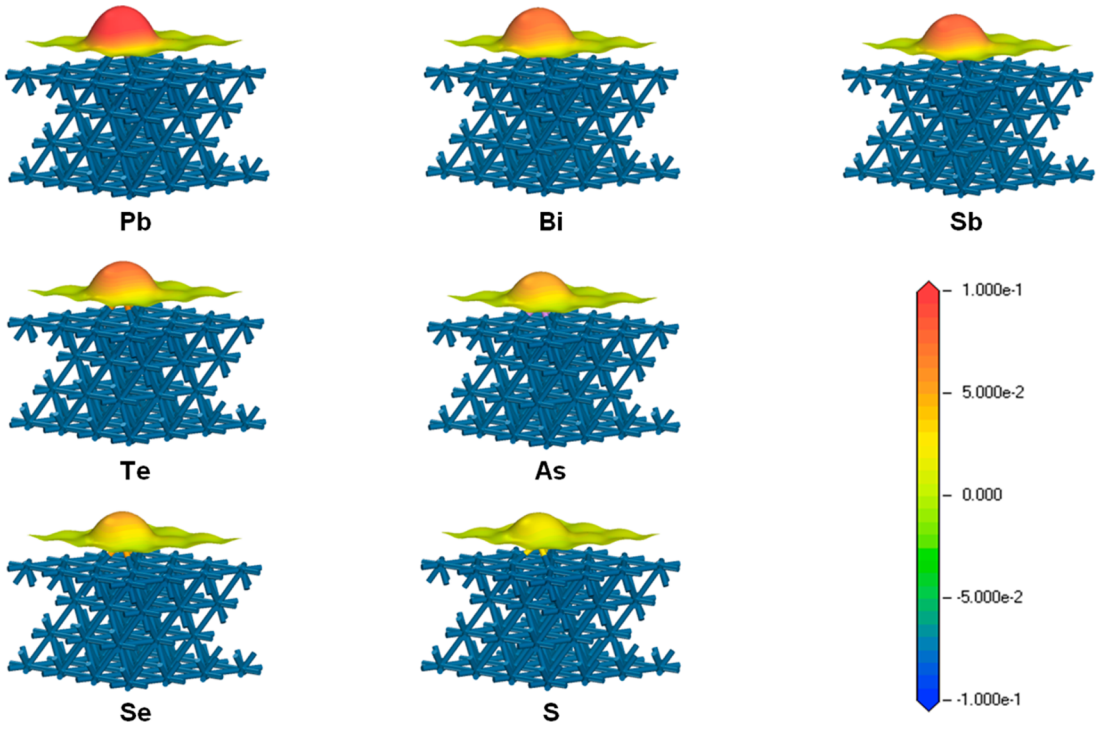

Figure 1. Electrostatic potential (Ha/e) mapped on the electron isodensity surface for a density value ρ = 0.01 e/Å^3 for Pb, Bi, Sb, Te, As, Se, and S adatoms adsorbed on the Pt(111) surface.

Table 2. Electronegativities and DFT Calculated Partial Charges under Two Different Formalisms for Different Adatoms Deposited on an fcc Site of the Pt(111) Surface

		adatom charge/e	
	electronegativity (Pauling)	Mulliken	Hirshfeld
Pb	1.87	0.64	0.40
Bi	2.02	0.50	0.32
Sb	2.05	0.41	0.27
Te	2.10	0.28	0.20
As	2.18	0.18	0.11
Pt	2.28	0.05	0.08
Se	2.55	0.02	0.06
S	2.58	−0.27	−0.02

is related to the partial positive charge appearing on the adatom.

Finally, for the investigated adatoms, Pauling electronegativities are also included in Table 2. From this table, a correlation between electronegativities and partial charges can be established. In fact, a linear relationship between the partial charge on the adatom (δ) and the electronegativity difference between the adatom and platinum (ΔE_N) is given in Figure 2. Additionally, it can also be observed that, for zero electronegativity difference, both models intercept the same 0.05 e value. Such a circumstance is consequence of the Smoluchowski effect.[59] This effect predicts some positive charge on the upper part of the defects of a surface, due to a redistribution of the charge that is not able to follow the geometrical profile. In fact, as can be observed in Table 2, a Pt adatom would have a positive partial charge between 0.05 and 0.08, depending on the formalism, a consequence of the aforementioned effect. Thus, the charge appearing on the adatom can be explained by the electronegativity difference between the adatom and Pt. Given the correlation between partial charge and catalytic activity, it

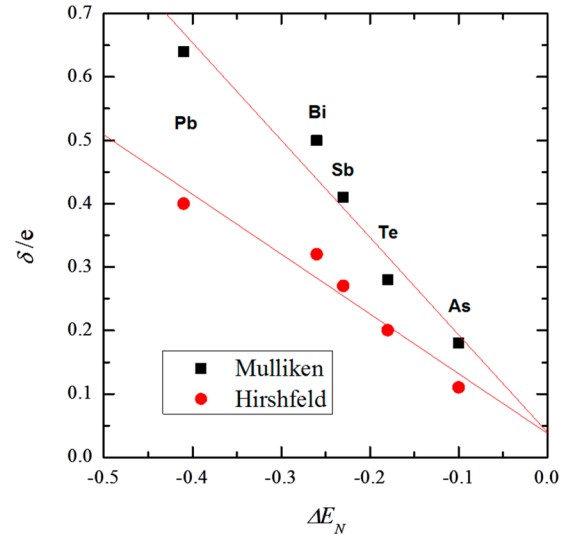

Figure 2. Partial charges (δ) vs difference in electronegativity between the adatom and platinum (ΔE_N) estimated under two different formalisms.

can be concluded that the electronegativity difference between the adatom and Pt can be used as a descriptor for the expected catalytic enhancement toward the formic acid oxidation reaction on the adatom-modified Pt(111) electrode.

Formic Acid Oxidation Mechanism. Since it was established that there exists a clear correlation between the positive charge located on the adatom upon adsorption on the Pt(111) surface and the formic acid oxidation currents measured experimentally, the precise effect of the adatom on the formic acid oxidation process was investigated. Several possibilities were considered. Formic acid (or formate) could interact first with the positively charged adatom and then react

DOI: 10.1021/cs501729j
ACS Catal. 2015, 5, 645−654

to yield CO_2. Alternatively, formic acid (or formate) could adsorb on the Pt atoms close to the adatom and from that state evolve to yield the final product. Using experimental and DFT results, here it is demonstrated that the most favorable mechanism proceeds through adsorption on the adatom: that is, the adatom plays an active role in the oxidation mechanism.

For the mechanism in which the adatom plays an active role, the effect of the adatom partial positive charge on the formic acid molecules approaching the surface was considered first. Physisorption energies of a hydrated formic acid molecule adsorbed near the different adatoms, in the configuration with the carbonyl group close to the adatom, are summarized in Table 3. In spite of the fact that, for the classical functionals, DFT is not the most accurate method in order to capture relatively weak interactions, the results presented in Table 3 suggest that the physisorption of hydrated formic acid on the adatom-modified surfaces is significant and that the interactions are strong enough as to be sufficiently captured by a classical functional. Additionally, it can be observed that the estimated physisorption energies are proportional to the positive charge located on the adatoms given in Table 2. Also, it was determined that, for the adatoms with a large partial positive charge (i.e., Bi and Pb), the interaction with the carbonyl group is more favorable, as was previously shown for Sb.[57] For the rest of the adatoms, the differences in energy between both configurations are within the error of the calculations. As expected, the distances between the formic acid molecule and the adatom become shorter as the positive change in the adatom increases (Figure 3), since there is a clear interaction of the partial negative charge of the carbonyl group and the positive charge of the adatom. Moreover, the physisorption of the formic acid molecule on the adatom also involves some structural changes in the hydrated formic acid ensemble, with changes in the distances of O−H bond and the hydrogen bond with respect to those calculated in the absence of the surface.

Table 3. DFT Calculated Physiorption Energies for a Hydrated Formic Acid Molecule on the Adatom-Modified Pt(111) Surface and the Distance between the Adatom and the O Atom of the Carbonyl Group in the Formic Acid Molecule

	distance/Å	energy/eV
Pb	3.26	−0.27
Bi	3.07	−0.26
Sb	3.36	−0.21
Te	3.69	−0.21
As	3.82	−0.19

From the described physisorbed configuration, the formic acid molecule may evolve to chemisorbed formate by deprotonation toward the solution. The positive charge on the adatom (Figure 1) would be the driving force of such a formate chemisorption process in two different ways. On one side, given that positive charges interact favorably with anions, the adatom would become an attractor for the conjugated base of the formic acid. On the other hand, the positive charge on the adatom would drive the chemisorption process of formate toward the adatom instead of platinum. At this solution pH, that is, when pH < pK_a, the average number of acid molecules at any given time is larger than those of the conjugated base, but there is a continuous and dynamic exchange between both forms, as in any other equilibria. Each time a formic acid molecule close to the adatom initiates the deprotonation process, the positive charge on the adatom would increase the probability that the molecule can be finally deprotonated and adsorbed on the adatom. Actually, from the formic acid physisorbed configuration, deprotonation and formate chemisorption process on the adatom would take place simultaneously, as DFT calculations corroborate. Due to the large positive charge located on some adatoms (see Table 2), adsorption of formate on the adatoms is energetically favorable and occurs in a barrierless process, where formate would be bonded to adatoms through an oxygen atom (Figure 4A). Moreover, running quantum mechanics molecular dynamic simulations, it was found that, in this chemisorbed mode, the formate fragment can rotate freely using the adatom−oxygen and contiguous oxygen−carbon bonds as rotation axes. Two major configurations were identified, in which there is a clear interaction with the surface: that with the C−H bond pointing to the surface (C−H down configuration, Figure 4A) and that with the C−H bond in the opposite direction (C−H up configuration). For all of the adatoms, the energy difference between both configurations is below 0.1 eV, which clearly indicates that the molecule can rotate freely, because all other configurations have energies between these two extreme values.

Finally, in order to yield CO_2, from the assumed formate chemisorption state on the adatom, the C−H bond should be

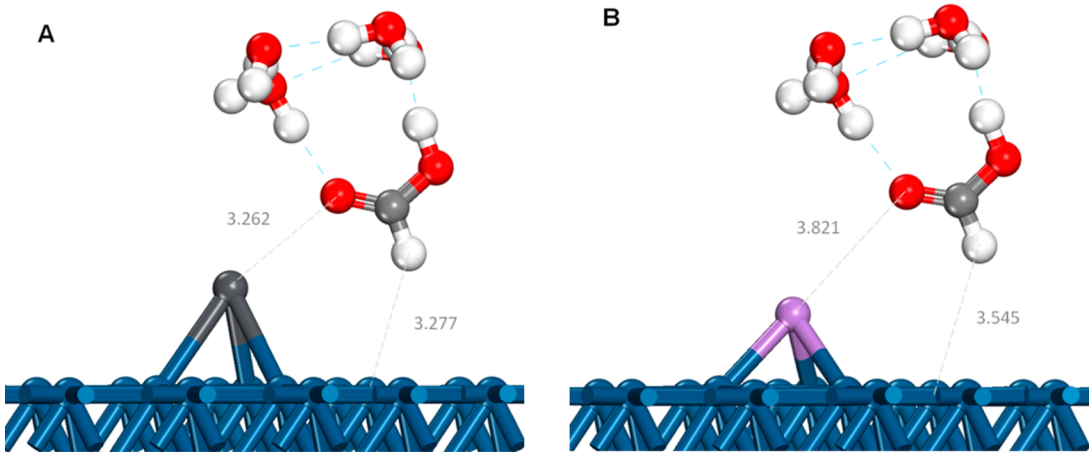

Figure 3. Physisorbed geometries of hydrated formic acid molecules on (A) Pb- and (B) As-modified Pt(111) surfaces.

DOI: 10.1021/cs501729j
ACS Catal. 2015, 5, 645−654

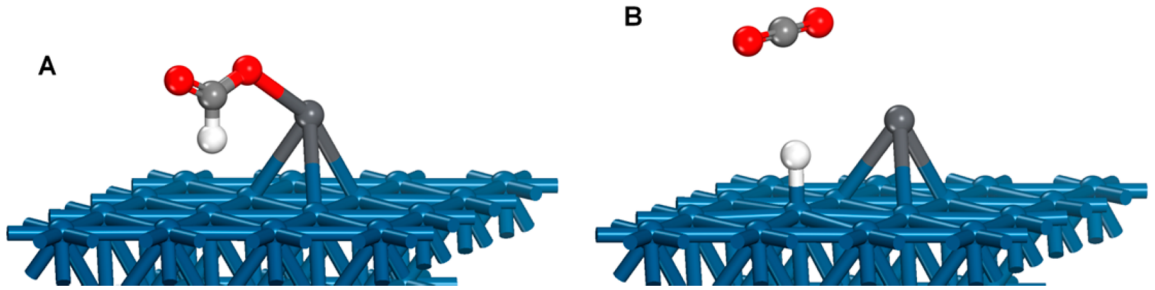

Figure 4. Geometries of (A) the HCOO fragment chemisorbed on the Pb−Pt(111) surface and (B) the final products yielded from the formic acid oxidation.

cleaved. For this last step of the whole process, the identified C−H down configuration is the relevant one. Taking into account the large affinity of platinum for hydrogen, it is possible that C−H bond cleavage takes place from such a configuration, in which the hydrogen atom is close to a Pt site. Moreover, it has been shown that the activation energy for the cleavage of the C−H bond on a Pt(111) surface from a C−H down configuration is significantly smaller than that measured for a C−H up configuration.[60] Thus, the energetics of the C−H bond cleavage schematized in Figure 4 was computed for all of the adatoms. For all cases, the resulting energy of the process was found to be favorable, and in most cases barrierless (Table 4), which indicates that the evolution of the adsorbed fragment

Table 4. DFT Calculated Activation Energies for the Cleavage of the C−H Bond from the Chemisorbed HCOO Fragment on the Adatom and the Total Energy of the Process[a]

	activation barrier/eV	energy/eV
Pb	dh	−1.03
Bi	dh	−1.25
Sb	0.11	−1.24
Te	dh	−1.59
As	0.09	−1.53

[a]Negligible activation energy is denoted as "dh".

to yield CO_2 is a favorable process for the adatoms that have a positive partial charge when they are adsorbed on Pt(111) surfaces. The total energy of this last step is less favorable as the partial positive charge of the adatom increases, although in all cases the process is clearly favorable. This is just a consequence of the difference in the adsorption energy of formate on the adatom. As the global process should have the same energy independently of the nature of the adatom, the adsorption energy of formate is more favorable as the partial positive charge on the adatom is larger, so that the energy released in the last step diminishes.

Having stablished that the mechanism under which the adatom adsorbs the HCOO fragment and the neighboring Pt atom helps in the cleavage of the C−H bond is almost a barrierless mechanism (the only expected energy barrier is deprotonation of the physisorbed formate molecule), the alternative mechanism involving the adsorption of formate on the Pt sites close to the adatom should be analyzed. In all of the reported mechanisms for Pt surfaces, monodentate and bidentate adsorbed formate are key intermediate species.[61,62] Thus, the adsorption energy of monodentate and bidentate formate ($HCOO_m$ and $HCOO_b$, respectively) adsorbed near the adatom on the Bi-modified Pt(111) surface and on the unmodified Pt surface were estimated. From all the considered adsorption processes, the adsorption of $HCOO_b$ on the unmodified surface is the most stable. Table 5 reports those

Table 5. DFT Calculated Adsorption Energies for $HCOO_m$ and $HCOO_b$ on Unmodified and Bi-Modified Pt(111) Surfaces, using the Adsorption Energy of $HCOO_b$ on the Unmodified Pt(111) Surface as Reference

species	ΔE/eV
$HCOO_m$ on Pt(111)	0.58
$HCOO_b$ on Bi−Pt(111)	0.17
$HCOO_m$ on Bi−Pt(111)	0.44

energies using the adsorption energy of $HCOO_b$ on the unmodified Pt(111) surface as reference. As can be seen, the adsorption of $HCOO_b$ on the Pt sites close to the Bi is ca. 0.17 eV less favorable than that estimated for the bare Pt(111) surface. This result is in very good agreement with the experimental behavior of adsorbed formate on Bi-modified Pt(111) surfaces inferred from fast voltammetry.[63] The onset for formate adsorption is displaced ca. 0.2 V for θ_{Bi} = 0.12, which is a coverage very similar to that corresponding to the calculations. In addition, the difference in adsorption energy between $HCOO_m$ and $HCOO_b$ for the unmodified Pt(111) surface is in good agreement with reported results.[61] In fact, the less favorable adsorption of formate on the adatom-modified surfaces can be also considered a consequence of the charge redistribution originating in the adsorption of the adatom. Due to the positive charge on the adatom, the Pt atoms have a partial negative charge, which hinders the adsorption of nucleophilic species, such as formate.

For a mechanism in which the adatom only modifies the energy of the neighboring Pt sites, that is, it is not involved directly in the catalysis, the lower adsorption energy of formate on the Pt sites close to the adatom will lead to higher barriers and therefore to lower current densities, as the results on the Pt(111) surface demonstrate.[61] It should be stressed that the calculated energy barriers for the whole mechanism on the unmodified Pt(111) surface are well above 0.5 eV,[61] whereas the mechanism in which formate is adsorbed on the adatom is almost barrierless.

The participation of the adatom in the mechanism by aiding in the C−H cleavage when the HCOO fragment is adsorbed in a neighboring Pt can also be discarded. It has been shown that the cleavage of the C−H bond in the $HCOO_b$ configuration on Pt(111) has a very high barrier (ca. 1 eV).[60] In this configuration, due to geometrical reasons, the interaction of the C−H bond with the adatom will be small, so that the activation barrier will continue to be very high. Lower activation

DOI: 10.1021/cs501729j
ACS Catal. 2015, 5, 645−654

barriers for the C−H cleavage on unmodified Pt(111) surfaces have been calculated from the $HCOO_m$ configuration.[61] However, the energy difference between the $HCOO_b$ and the $HCOO_m$ adsorption modes in Bi−Pt(111) surfaces is 0.27 eV, and the energy barrier for the transition will be higher. In comparison with the mechanism where the adatom adsorbs the HCOO fragment, this process is less favorable even without considering the barrier for C−H bond cleavage, since it already has higher barriers. Moreover, the energy barriers for the cleavage of the C−H bond from $HCOO_m$ are not expected to be negligible. In the most favorable mechanism, the partial positive charge of the adatom favors the adsorption of the anion and the affinity of platinum for hydrogen adsorption helps in C−H bond cleavage. In the mechanism initiated by the adsorption on platinum, formate is adsorbed in a less favorable site (due to the negative charge compensating the positive charge located on the adatom) and the cleavage of the C−H bond is occurring on an adatom with lower hydrogen affinity. As a conclusion, the mechanism involving the adsorption of HCOO fragments on Pt cannot explain the enhanced catalytic activity observed.

In summary, the proposed oxidation mechanism of formic acid on adatom-modified Pt(111) surfaces in which formic acid interacts first with the adatom is consistent with the experimental observation that adatoms catalyze the oxidation process, the adatom−Pt ensemble being the most active site. In fact, the computational results described above indicate that the catalysis occurs through a bifunctional mechanism, in which distinct roles are played by the adatom and a Pt site close to the adatom, forming an adatom−Pt ensemble. Adatoms having electronegativity lower than that of platinum give rise to a partial positive charge on the adatom when they are adsorbed. The positive charge on the adatom attracts the formic acid molecule toward the adatom, and a physisorption phenomenon takes place. From such a physisorbed state, formic acid can deprotonate to give the formate anion, which is immediately chemisorbed on the adatom. Once chemisorbed, the formate fragment rotates freely around the adatom−O and contiguous O−C bonds until a sufficiently favorable C−H down configuration is reached. Finally, from such a configuration, the C−H bond is cleaved, yielding CO_2 as a product. According to the computed mechanism, all of the identified steps are virtually barrierless except for the deprotonation of the formic acid molecule, which clearly has some barrier involved at acidic pH values.

Experimental Verification of the Proposed Mechanism. With the goal in mind of verifying the proposed formic acid oxidation mechanism, new voltammetric experiments on the Bi−Pt(111) system were conducted for three different bismuth coverages and the bare surface (Figure 5). In the absence of formic acid, three different regions, corresponding to three different processes occurring on the surface, can be identified in the voltammetric profiles for the modified electrodes in sulfuric acid solutions (Figure 5A). At 0.06 V, the platinum sites are covered by adsorbed hydrogen, which is desorbed between this potential and 0.2−0.3 V depending on the coverage. Between 0.3 and 0.5 V, sulfate is adsorbed on the available Pt sites and the adsorption/desorption process gives rise to the signal in this region. The last region, with the peak centered at 0.62 V, is related to the OH adsorption on the bismuth adatoms.

The same three different regions can also be identified in the voltammogram recorded for the oxidation of formic acid

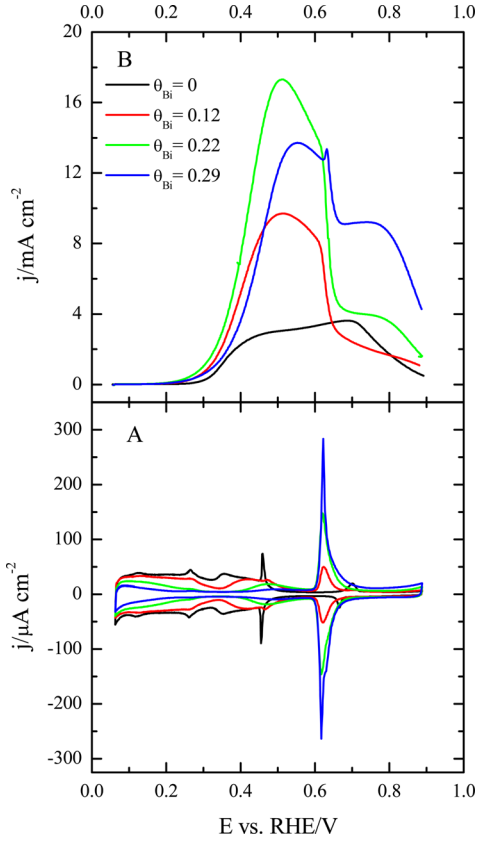

Figure 5. Voltammetric profiles for the Bi−Pt(111) electrode for different bismuth coverages in (A) a 0.5 M H_2SO_4 solution and (B) a 0.5 M H_2SO_4 + 0.1 M HCOOH solution at 25 °C. Scan rate: 50 mV s^{-1}.

(Figure 5B). In the region where hydrogen is adsorbed, no oxidation currents are detected. The onset for the oxidation of formic acid coincides with the final desorption of hydrogen from the Pt sites. It should be highlighted that the displacement of the onset for the formic acid oxidation toward lower potential values as the adatom coverage increases is parallel to the displacement of the final stages of the hydrogen desorption. This fact is in agreement with the oxidation mechanism proposed by DFT. In the final step of the process, the cleavage of the C−H bond yields an adsorbed H atom on Pt, which should be desorbed for the reaction to continue. Since the oxidation reaction is not possible in a hydrogen-covered surface, the reaction can only proceed at potentials where hydrogen desorption is a spontaneous process. From the onset potential, the oxidation current increases up to 0.5 V, where it reaches a maximum, and at 0.6−0.62 V the current abruptly diminishes to reach very low values. The abrupt diminution coincides with the potential where the adsorption of OH occurs on the Bi adatom. This fact is also in agreement with the proposed mechanism, since the adsorption of OH will hinder the adsorption of formate, blocking the reaction. Thus, it can be proposed that H adsorption on platinum and OH adsorption on bismuth act as inhibitors of the reaction.

As mentioned earlier, our DFT results suggest that the activation barriers on Pb- or Bi-modified Pt(111) electrodes would be clearly lower than those operating on the bare surface. Thus, a significant diminution of the experimental activation energy for the modified electrodes should be measured. Given that, on these modified electrodes, the formic acid oxidation

DOI: 10.1021/cs501729j
ACS Catal. 2015, 5, 645−654

reaction occurs exclusively through the active intermediate route, voltammetry can be used directly to determine the activity through this route. Voltammograms at five temperatures for a Bi−Pt(111) electrode with θ_{Bi} = 0.12 are displayed in Figure 6. As can be seen, the hysteresis between the positive

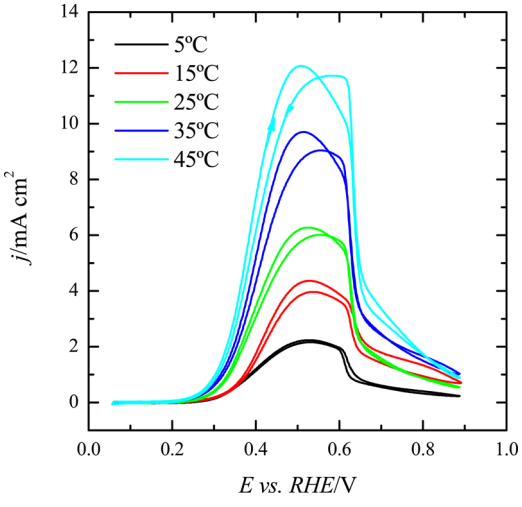

Figure 6. Voltammetric profiles for the Bi−Pt(111) electrode with θ_{Bi} = 0.12 in a 0.5 M H_2SO_4 + 0.1 M HCOOH solution at different temperatures. Scan rate: 50 mV s^{-1}.

and negative scans is very small, which confirms that the formation of CO is negligible. In fact, currents in the positive scan direction are larger than those measured in the negative direction. From these measurements, activation energies can be calculated from Arrhenius plots, as shown in ref 64. Such activation energies are plotted and compared to that measured for the Pt(111) electrode in Figure 7. For the unmodified Pt(111) electrode, data has been taken from ref 64, in which the activation energy has been calculated using pulsed voltammetry to separate the contribution from the active intermediate route from those related to the CO formation. As shown in Figure 7, a clear diminution of the experimental activation energy is observed as the bismuth coverage increases.

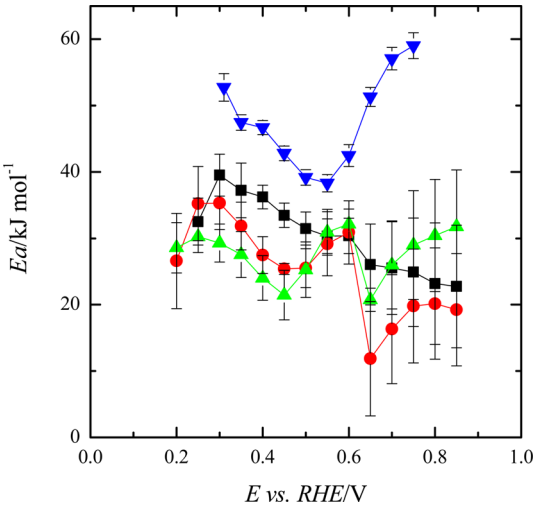

Figure 7. Measured activation energies at different potentials for different Bi coverages on the Pt(111) electrode: (▼) θ_{Bi} = 0.00; (■) θ_{Bi} = 0.12; (●) θ_{Bi} = 0.22; (▲) θ_{Bi} = 0.28.

For the modified electrodes, three different regions can be identified in the activation energy plot vs electrode potential. From the onset of the oxidation (ca. 0.2−0.3 V depending on the adatom coverage; see Figure 5B), the activation energy diminishes until a minimum value is reached at ca. 0.5 V. Between 0.5 and 0.7 V, the region in which the redox process of the Bi adatom takes place, there is a sudden change in the activation energy. As mentioned earlier, at ca. 0.6 V, there is an abrupt diminution of the current linked to the adsorption of OH on the adatom that blocks the adsorption of formate. Since this process is affected by temperature,[65] the exact potential where the sharp diminution occurs is also influenced by temperature. Thus, the apparent activation energy measured in this region is then a consequence of the effect of the temperature in the OH adsorption process on the adatom and is not directly related to the formic acid oxidation reaction. At higher potentials, the currents are very low and the measured activation energy has a significant error.

In the region between 0.3 and 0.5 V, the experimental activation energy contains the contribution of Pt−Bi ensembles, where the reaction proceeds through the mechanism proposed in this paper, and the Pt−Pt ensembles, where the reaction proceeds according to the mechanism proposed in ref 64. The experimental activation energy for the Pt(111) electrode with θ_{Bi} = 0.28 is 21 kJ mol^{-1}, whereas the corresponding activation energy on the unmodified Pt(111) electrode at the same potential is 42 kJ mol^{-1}. This fact implies that the activation energy has been reduced by half and the measured currents have increased more than 1 order of magnitude.

According to the DFT calculations, even lower activation energy values should have been expected. However, in a mechanism where activation barriers are small and, therefore, there is no clear rate-determining step, the experimental activation energy should contain the contributions from all of the steps. In the proposed mechanism two steps clearly contribute. The first is the deprotonation of the formic acid to yield formate, since it is a step which has an unfavorable energy. Assuming that the acid constant of formic acid in the interphase is the same as that measured in the bulk, the corresponding free energy for the deprotonation process in a 0.5 M H_2SO_4 solution (pH close to 0.3) is ca. 9 kJ mol^{-1}. The second contribution to the activation energy is located at low potentials, related to the hydrogen desorption process required to liberate the adsorption site and to reestablish the surface to the initial conditions. The observed diminution of the activation energy between 0.3 and 0.5 V can be related to this process. Thus, as the potential increases, hydrogen desorption is more favorable, diminishing all the measured activation energy of the reaction. Probably at 0.5 V the contribution of this step is negligible.

The measured activation energy is higher than those values. However, it should be taken into account that the experimental values do not only contain information on the activation energy of the whole reaction on the Pt−Bi ensemble. As mentioned earlier, Pt−Pt ensembles also contribute to the measured activation energy, although their number at high bismuth coverages is small.[63] Additionally, the dependence on the temperature of all the adsorption processes that take place in the mechanism or are competing for the adsorption sites also contributes to the measured activation energy, as shown for the oxidation on the unmodified Pt(111) electrode.[64] All of these factors increase the measured activation energy.

DOI: 10.1021/cs501729j
ACS Catal. 2015, 5, 645−654

CONCLUSIONS

Experimental results show that certain adatoms increase the catalytic activity of Pt(111) electrodes toward the formic acid oxidation reaction. Here, with the support of a combination of computational and experimental results, an explanation for such an observation has been provided for the first time. More specifically, the oxidation mechanism of formic acid on Pt(111) electrodes modified by adatoms of the p block has been revealed. The charge redistribution occurring as a consequence of the adatom adsorption process drives the oxidation process. A direct correlation between the positive charge located on the adatom and the activity of the modified electrode has been found. Moreover, such a partial positive charge is proportional to the difference in electronegativity between the adatom and platinum, and therefore the electronegativity difference is an excellent descriptor of the expected electrocatalytic activity of the modified surface toward the reaction. Additionally, this partial positive charge is the key factor that drives the oxidation mechanism. It favors the physisorption of formic acid near the adatom and also its deprotonation and further chemisorption, on the adatom, in formate form. In the chemisorbed formate state, the HCOO fragment can rotate freely and, when the H atom is close to a neighboring platinum atom, the cleavage of the C−H bond occurs to yield a CO_2 molecule and an adsorbed hydrogen atom. The final step in the process can be considered to be the desorption of the H atom. Thus, the oxidation mechanism proposed here can be described as a bifunctional mechanism, in which adatoms favor the formation and adsorption of formate and platinum is in charge of the cleavage of the C−H bond. Additionally, for the proposed mechanism, a clear diminution of the activation energy with respect to that operating on the unmodified electrode is computationally predicted and experimentally corroborated.

AUTHOR INFORMATION

Corresponding Author

*E-mail for E.H.: herrero@ua.es.

Notes

The authors declare no competing financial interest.

ACKNOWLEDGMENTS

This work has been financially supported by the MINECO (Spain) (project CTQ2013-44083-P) and Generalitat Valenciana (project PROMETEOII/2014/013).

REFERENCES

(1) Parsons, R. *Trans. Faraday Soc.* **1958**, *54*, 1053−1063.
(2) Conway, B. E.; Bockris, J. O. *J. Chem. Phys.* **1957**, *26*, 532−541.
(3) Trasatti, S. *J. Electroanal. Chem.* **1972**, *39*, 163−184.
(4) Trasatti, S. *J. Chem. Soc., Faraday Trans. I* **1972**, *68*, 229−236.
(5) Greeley, J.; Jaramillo, T. F.; Bonde, J.; Chorkendorff, I. B.; Norskov, J. K. *Nat. Mater.* **2006**, *5*, 909−913.
(6) Stephens, I. E. L.; Bondarenko, A. S.; Gronbjerg, U.; Rossmeisl, J.; Chorkendorff, I. *Energy Environ. Sci.* **2012**, *5*, 6744−6762.
(7) Parsons, R.; Vandernoot, T. *J. Electroanal. Chem.* **1988**, *257*, 9−45.
(8) Willsau, J.; Heitbaum, J. *Electrochim. Acta* **1986**, *31*, 943−948.
(9) Clavilier, J.; Parsons, R.; Durand, R.; Lamy, C.; Leger, J. M. *J. Electroanal. Chem.* **1981**, *124*, 321−326.
(10) Sun, S. G.; Clavilier, J.; Bewick, A. *J. Electroanal. Chem.* **1988**, *240*, 147−159.
(11) Grozovski, V.; Climent, V.; Herrero, E.; Feliu, J. M. *ChemPhysChem* **2009**, *10*, 1922−1926.
(12) Grozovski, V.; Climent, V.; Herrero, E.; Feliu, J. M. *Phys. Chem. Chem. Phys.* **2010**, *12*, 8822−8831.
(13) Watanabe, M.; Horiuchi, M.; Motoo, S. *J. Electroanal. Chem.* **1988**, *250*, 117−125.
(14) Clavilier, J.; Fernández-Vega, A.; Feliu, J. M.; Aldaz, A. *J. Electroanal. Chem.* **1989**, *261*, 113−125.
(15) Clavilier, J.; Fernández-Vega, A.; Feliu, J. M.; Aldaz, A. *J. Electroanal. Chem.* **1989**, *258*, 89−100.
(16) Fernández-Vega, A.; Feliu, J. M.; Aldaz, A.; Clavilier, J. *J. Electroanal. Chem.* **1989**, *258*, 101−113.
(17) Fernández-Vega, A.; Feliu, J. M.; Aldaz, A.; Clavilier, J. *J. Electroanal. Chem.* **1991**, *305*, 229−240.
(18) Herrero, E.; Fernández-Vega, A.; Feliu, J. M.; Aldaz, A. *J. Electroanal. Chem.* **1993**, *350*, 73−88.
(19) Xia, X. H.; Iwasita, T. *J. Electrochem. Soc.* **1993**, *140*, 2559−2565.
(20) Llorca, M. J.; Herrero, E.; Feliu, J. M.; Aldaz, A. *J. Electroanal. Chem.* **1994**, *373*, 217−225.
(21) Herrero, E.; Llorca, M. J.; Feliu, J. M.; Aldaz, A. *J. Electroanal. Chem.* **1995**, *394*, 161−167.
(22) Lei, H. W.; Hattori, H.; Kita, H. *Electrochim. Acta* **1996**, *41*, 1619−1628.
(23) Climent, V.; Herrero, E.; Feliu, J. M. *Electrochim. Acta* **1998**, *44*, 1403−1414.
(24) Smith, S. P. E.; Ben-Dor, K. F.; Abruna, H. D. *Langmuir* **1999**, *15*, 7325−7332.
(25) Smith, S. P. E.; Abruna, H. D. *J. Electroanal. Chem.* **1999**, *467*, 43−49.
(26) Maciá, M. D.; Herrero, E.; Feliu, J. M. *J. Electroanal. Chem.* **2003**, *554*, 25−34.
(27) Buso-Rogero, C.; Perales-Rondon, J. V.; Farias, M. J. S.; Vidal-Iglesias, F. J.; Solla-Gullon, J.; Herrero, E.; Feliu, J. M. *Phys. Chem. Chem. Phys.* **2014**, *16*, 13616−13624.
(28) Llorca, M. J.; Feliu, J. M.; Aldaz, A.; Clavilier, J. *J. Electroanal. Chem.* **1994**, *376*, 151−160.
(29) Baldauf, M.; Kolb, D. M. *J. Phys. Chem.* **1996**, *100*, 11375−11381.
(30) Kibler, L. A.; El-Aziz, A. M.; Hoyer, R.; Kolb, D. M. *Angew. Chem., Int. Ed.* **2005**, *44*, 2080−2084.
(31) Casado-Rivera, E.; Gal, Z.; Angelo, A. C. D.; Lind, C.; DiSalvo, F. J.; Abruna, H. D. *ChemPhysChem* **2003**, *4*, 193−199.
(32) Roychowdhury, C.; Matsumoto, F.; Mutolo, P. F.; Abruna, H. D.; DiSalvo, F. J. *Chem. Mater.* **2005**, *17*, 5871−5876.
(33) Blasini, D. R.; Rochefort, D.; Fachini, E.; Alden, L. R.; DiSalvo, F. J.; Cabrera, C. R.; Abruna, H. D. *Surf. Sci.* **2006**, *600*, 2670−2680.
(34) Alden, L. R.; Han, D. K.; Matsumoto, F.; Abruña, H. D.; DiSalvo, F. J. *Chem. Mater.* **2006**, *18*, 5591−5596.
(35) Matsumoto, F.; Roychowdhury, C.; DiSalvo, F. J.; Abruna, H. D. *J. Electrochem. Soc.* **2008**, *155*, B148−B154.
(36) Clavilier, J.; Armand, D.; Sun, S. G.; Petit, M. *J. Electroanal. Chem.* **1986**, *205*, 267−277.
(37) Korzeniewski, C.; Climent, V.; Feliu, J. M. In *Electroanalytical chemistry: A series of advances*; Bard, A. J., Zoski, C., Eds.; CRC Press: Boca Raton, FL, 2012; Vol. *24*, pp 75−169.
(38) Rodes, A.; Elachi, K.; Zamakhchari, M. A.; Clavilier, J. *J. Electroanal. Chem.* **1990**, *284*, 245−253.
(39) Itaya, K.; Sugawara, S.; Sashikata, K.; Furuya, N. *J. Vac. Sci. Technol. A* **1990**, *8*, 515−519.
(40) Gomez-Marin, A. M.; Feliu, J. M. *Electrochim. Acta* **2012**, *82*, 558−569.
(41) Clavilier, J.; Feliu, J. M.; Aldaz, A. *J. Electroanal. Chem.* **1988**, *243*, 419−433.
(42) Garcia-Araez, N.; Climent, V.; Feliu, J. In *Interfacial phenomena in electrocatalysis*; Vayenas, C. G., Ed.; Springer: New York, 2011; Vol. *51*, pp 1−105.
(43) Delley, B. *J. Chem. Phys.* **1990**, *92*, 508−517.
(44) Delley, B. *Phys. Rev. B* **2002**, *66*, 155125.
(45) Hammer, B.; Hansen, L. B.; Nørskov, J. K. *Phys. Rev. B* **1999**, *59*, 7413−7421.
(46) Delley, B. *J. Chem. Phys.* **2000**, *113*, 7756−7764.

DOI: 10.1021/cs501729j
ACS Catal. 2015, 5, 645−654

(47) Delley, B. *Mol. Simul.* **2006**, *32*, 117−123.
(48) Neugebauer, J.; Scheffler, M. *Phys. Rev. B* **1992**, *46*, 16067−16080.
(49) Monkhorst, H. J.; Pack, J. D. *Phys. Rev. B* **1976**, *13*, 5188−5192.
(50) Maciá, M. D.; Herrero, E.; Feliu, J. M.; Aldaz, A. *Electrochem. Commun.* **1999**, *1*, 87−89.
(51) Maciá, M. D.; Herrero, E.; Feliu, J. M.; Aldaz, A. *J. Electroanal. Chem.* **2001**, *500*, 498−509.
(52) Herrero, E.; Climent, V.; Feliu, J. M. *Electrochem. Commun.* **2000**, *2*, 636−640.
(53) Leiva, E.; Iwasita, T.; Herrero, E.; Feliu, J. M. *Langmuir* **1997**, *13*, 6287−6293.
(54) Kim, J.; Rhee, C. K. *Electrochem. Commun.* **2010**, *12*, 1731−1733.
(55) Mulliken, R. S. *J. Chem. Phys.* **1955**, *23*, 1833−1840.
(56) Hirshfeld, F. L. *Theor. Chim. Acta* **1977**, *44*, 129−138.
(57) Peng, B.; Wang, H.-F.; Liu, Z.-P.; Cai, W.-B. *J. Phys. Chem. C* **2010**, *114*, 3102−3107.
(58) Lin, W. F.; Sun, S. G.; Tian, Z. W. *J. Electroanal. Chem.* **1994**, *364*, 1−7.
(59) Smoluchowski, R. *Phys. Rev.* **1941**, *60*, 661−674.
(60) Wang, H.-F.; Liu, Z.-P. *J. Phys. Chem. C* **2009**, *113*, 17502−17508.
(61) Gao, W.; Keith, J. A.; Anton, J.; Jacob, T. *J. Am. Chem. Soc.* **2010**, *132*, 18377−18385.
(62) Neurock, M.; Janik, M.; Wieckowski, A. *Faraday Discuss.* **2009**, *140*, 363−378.
(63) Perales-Rondón, J. V.; Ferre-Vilaplana, A.; Feliu, J. M.; Herrero, E. *J. Am. Chem. Soc.* **2014**, *136*, 13110−13113.
(64) Perales-Rondón, J. V.; Herrero, E.; Feliu, J. M. *Electrochim. Acta* **2014**, *140*, 511−517.
(65) Blais, S.; Jerkiewicz, G.; Herrero, E.; Feliu, J. M. *J. Electroanal. Chem.* **2002**, *519*, 111−122.

DOI: 10.1021/cs501729j
ACS Catal. 2015, 5, 645−654